

Validation of Global Illumination Simulations through CCD Camera Measurements

*Sumanta N. Pattanaik, James A. Ferwerda,
Kenneth E. Torrance and Donald Greenberg
Program of Computer Graphics
Cornell University
Ithaca, NY-14853, USA*

Abstract

In this paper we present a technique for calibrating a CCD camera for direct colorimetric comparison between the captured images of the real environment and synthetic images of the simulated environments. We use this comparison to validate lighting simulation algorithms used for computing synthetic images.

1. Introduction

For nearly 25 years one of the main research efforts at the Cornell Program of Computer Graphics has been the development of algorithms for physically accurate simulation of light transport in environments [Goral84, Cohen86, Sillion91, Smits94, Walter97]. Given the geometry of the physical scene, and the spectral and directional surface reflectance and emittance values of surfaces, these algorithms can compute the spectral radiance at any point in the scene. If these algorithms are to become predictive then it is important to validate the results computed by these algorithms with experimental comparisons. To carry out experimental comparisons we have set up a light measurement laboratory which includes a calibrated integrating sphere light source and a scientific grade CCD camera for measuring the light.

In this paper we will first discuss the methods we have used to colorimetrically and radiometrically calibrate our CCD camera to allow it to be used to acquire accurate measurements of light energy from any environment. Using these measurements we will then show the results of direct colorimetric comparisons between the physical environment and global illumination simulations of it. We hope that the results of these studies will provide a new standard methodology for physically-based image synthesis.

2. CCD Camera Calibration

In order to use our CCD camera for light measurement we need to determine the relationship of the CCD output to the

incident light and to the various camera parameters, such as exposure time, focal settings, aperture sizes, electronic noise *etc.*. By understanding this relationship we can then derive quantitative colorimetric and radiometric information about the incident light. We approached this calibration through the mathematical models described below.

The particular CCD camera we used is the Photometrics PXL 1300. It utilizes a liquid-cooled Kodak KAF1300L scientific grade CCD image sensor which contains a 2-D array of sensor elements.

2.1. Noise Correction

There are two types of noise associated with CCD imaging systems: additive noise and multiplicative noise.

Additive Noise: In addition to the action of light, thermal agitation gives rise to charges inside the sensor element. These charges are indistinguishable from those generated by light. It is possible to reduce thermal noise by deeply cooling the CCD imager. Another form of additive noise is *preamplifier noise*, which is generated by the on-chip output amplifier. This noise is always present. A simple and efficient method of suppressing additive noise is to obtain the signal (S_d) in complete darkness, and subtract S_d from the original signal (S_o).

Multiplicative Noise: Multiplicative noise results from sensitivity variations between the sensors in the CCD imager. Correction of this noise requires the measurement of a correction frame or *flat field* (S_f) corresponding to a uniform field source.

The corrected signal S is given by:

$$S = (S_o - S_d) \frac{S_{fa}}{S_f - S_d} \quad (1)$$

where S_o is the measured signal and S_{fa} is the average signal of the flat field.

The CCD signal after noise correction is independent of the pixel position. Thus every pixel in the CCD imager may be considered to be independent.

2.2. Sensor Calibration

The CCD pixel signal is proportional to the number of photons incident on the sensor area. However, photons of different wavelength have different capacity to generate photoelectrons. The relationship between the pixel signal and the spectral distribution of the incident photons can be written as:

$$S \propto \int_{\lambda_a}^{\lambda_b} Q(\lambda) \cdot N_p(\lambda) \cdot d\lambda$$

where $Q(\lambda)$ is the quantal efficiency at wavelength λ , and $N_p(\lambda)$ is the number of photons of wavelength λ incident on the pixel.

Assuming that the light source has a constant emission over an exposure period, the number of photons at a wavelength λ falling on the sensor area is

$$N_p(\lambda) = t \cdot \mathcal{F}(\lambda) \cdot \int_{\text{Pixel_Area}} E(\lambda) \cdot dA \quad (2)$$

where $\mathcal{F}(\lambda)$ is the energy to quanta conversion factor and $E(\lambda)$ is the spectral irradiance. For an ideal optical system, irradiance of a differential area near the point where the principal axis meets the image plane can be expressed as

$$E(\lambda) = T(\lambda) \cdot L(\lambda) \cdot d^{-2} \cdot f^{-2}$$

where $T(\lambda)$ is the spectral transmittance of the optical system, $L(\lambda)$ is the spectral radiance of the emitting target, f is the F-stop and d is the image distance[Kingslake92]. For areas away from that point the irradiance expression can become very complicated. However for small apertures irradiance can be shown to differ by a multiplicative factor of $\cos^4 \alpha$ where α is equal to the angle between the differential area and the center of the aperture. This factor is compensated for during the flat field correction (Equation (1)) and hence the equation above may be considered to be valid over the whole imaging area.

Assuming the irradiance to be constant over the pixel area we can rewrite the expression for the photon count as:

$$N_p(\lambda) \propto t \cdot \mathcal{F}(\lambda) \cdot T(\lambda) \cdot L(\lambda) \cdot f^{-2} \cdot d^{-2} \cdot \text{Pixel_area}$$

and the expression for the signal generated at the pixel as:

$$S = C \cdot t \cdot f^{-2} \cdot d^{-2} \cdot \int_{\lambda_a}^{\lambda_b} \mathcal{F}(\lambda) \cdot Q(\lambda) \cdot T(\lambda) \cdot L(\lambda) \cdot d\lambda, \quad (3)$$

where C is a constant which subsumes the pixel area, the proportionality between the aperture area and F-stop, and the amplification factor related to the CCD circuitry.

2.3. Extraction of Colorimetric Information

The CCD signal modeled by Equation (3) does not provide any colorimetric information. In this section we describe

a method for computing colorimetric information from the CCD pixel signal.

The colorimetric quantities X , Y , and Z for a light source of spectral distribution $L(\lambda)$ are given by :

$$\begin{aligned} X &= \int_{\lambda_1}^{\lambda_2} L(\lambda) \bar{x}(\lambda) d\lambda; & Y &= \int_{\lambda_1}^{\lambda_2} L(\lambda) \bar{y}(\lambda) d\lambda; \\ Z &= \int_{\lambda_1}^{\lambda_2} L(\lambda) \bar{z}(\lambda) d\lambda, \end{aligned} \quad (4)$$

where $\bar{x}(\lambda)$, $\bar{y}(\lambda)$ and $\bar{z}(\lambda)$ are the CIE ideal observer color matching functions.

The equations imply that we have to know the target spectrum to compute the colorimetric values. However, we show below that it is possible to derive the colorimetric values of an unknown target by taking multiple measurements through narrow band filters.

A simplified expression for the CCD pixel value for measurement through a narrow band filter can be written as:

$$S_i = K \int_{\lambda_1}^{\lambda_2} L(\lambda) F_i(\lambda) d\lambda \quad (5)$$

where $K = C \cdot t \cdot f^{-2} \cdot d^{-2}$, $F_i(\lambda) = \mathcal{F}(\lambda) \cdot Q(\lambda) \cdot T_i(\lambda)$ and $T_i(\lambda)$ is the spectral transmittance of the camera lens and i -th narrow band filter.

Given sufficient narrow band filter and lens combinations we can express the color matching functions $\bar{x}(\lambda)$, $\bar{y}(\lambda)$ and $\bar{z}(\lambda)$ as linear combinations of $F_i(\lambda)$'s. *i.e.*

$$\begin{aligned} \bar{x}(\lambda) &\approx \sum_i b_i^x F_i(\lambda); & \bar{y}(\lambda) &\approx \sum_i b_i^y F_i(\lambda); \\ \bar{z}(\lambda) &\approx \sum_i b_i^z F_i(\lambda). \end{aligned}$$

Substituting these in Equation (4) we will get the expressions for X , Y and Z in terms of the CCD pixel signals. The resulting expression for X is given below.

$$\begin{aligned} X &\approx \int_{\lambda_1}^{\lambda_2} L(\lambda) \sum_i b_i^x F_i(\lambda) d\lambda \\ &= \sum_i b_i^x \int_{\lambda_1}^{\lambda_2} L(\lambda) F_i(\lambda) d\lambda = \frac{1}{K} \sum_i b_i^x S_i. \end{aligned}$$

We will get similar expressions for Y and Z . Thus from a linear combination of the CCD measurements taken through a set of narrow band filters we can compute the colorimetric values of a target. The accuracy of this computation will depend on how well the CIE matching functions are approximated by the narrow-band filter functions.

2.4. Verification of the Calibration Model

Using the CCD camera and an integrating sphere uniform light source we have tested our calibration model (Equation (3)) relating the pixel signal to various physical factors [Chen96]. Figure 1 shows the linear relationship of the pixel signal as a function of the exposure time. Figure 2 indicates the inverse square relationship between the measured signal and the F-Stop of the camera. Figure 3 establishes the inverse square relationship between the measured signal and the image distance. Figure 4 shows the linear relationship between the CCD signal and the photon density. We have computed the proportionality constant in Equation (3) from measurements of a known light source spectrum.

We used seven narrow band filters to compute colorimetric information from the CCD measurements. The transmittance of the filters are given in the Figure 5. Figure 6 shows the plot of the reconstructed $\bar{y}(\lambda)$ function and the actual $\bar{y}(\lambda)$.

3. Comparison Experiments

To perform our comparison experiment we took a simple environment consisting of a box with painted interior, a light source on the ceiling and two smaller boxes positioned on the floor. This physical environment is popularly known as the Cornell Box¹. We acquired bandpass images of the Cornell box using the CCD camera and the narrow band filters. Using the calibration model we then computed CIE tristimulus values for each image point of the real Cornell Box. Then we extracted the optical and geometrical camera viewing parameters using the camera calibration technique developed by Tsai [Tsai86]. We then used these camera parameters to render a synthetic image of the Cornell Box. Spectral values produced by the rendering algorithm were used to compute the CIE tristimulus values (X , Y , Z) for the comparison. Figure 7 shows the measured image, the simulated image and their luminance (Y) difference using pixel-wise comparison. Except for certain localized regions we find good correspondence between the simulated and the synthetic image. From the difference image we see that most of the mismatch is localized to the boundaries of the objects in the scene. We attribute most of this to the mismatch between the numerical description of the scene geometry and the actual geometry.

4. Discussion

We have presented techniques for calibrating a CCD camera to allow direct colorimetric and radiometric compar-

¹The geometry, reflection and emission data for the Cornell box is available on the web page <http://www.graphics.cornell.edu/cbox>.

isons between real environments and computer graphics simulations. We have used this calibrated camera to validate the colorimetric accuracy of physically based global illumination of rendering methods. We are currently performing radiometric calibration of the camera and plan to carry out full spectral comparisons between real environments and simulations. The results of these studies will provide an important standard methodology for physically based image synthesis.

5. Bibliography

- Chen96** Steve S-F. Chen, Jerry Wei-Chieh Li, Kenneth E. Torrance, Sumanta N. Pattanaik, *Preliminary Calibration of the Photometrics PXL1300L CCD Camera*, Technical report, no. PCG-96-1, Program of Computer Graphics, Cornell University, 1996.
- Cohen86** Michael Cohen, Donald P. Greenberg, Dave S. Immel, Philip J. Brock. *An Efficient Radiosity Approach for Realistic Image Synthesis*, IEEE Computer Graphics and Applications, vol 6(3), 1986, pp. 26-35.
- Goral84** Cindy M. Goral, Kenneth E. Torrance and Donald P. Greenberg. *Modeling the interaction of light between diffuse surfaces*. Proceedings of ACM SIGGRAPH, 1984, pp.213-222.
- Kingslake92** Rudolf Kingslake. *Optics in Photography*. SPIE Optical Engineering Press, Washington, 1992.
- Sillion91** Francois X. Sillion, James Arvo, Stephen Westin and Donald Greenberg, *A global illumination algorithm for general reflectance distributions*, Proceedings of ACM SIGGRAPH, 1991, pp.187-196.
- Smits94** Brian E. Smits, James R. Arvo, and Donald P. Greenberg. *A clustering algorithm for radiosity in complex environment*, Proceedings of ACM SIGGRAPH, 1994, pp.435-442.
- Tsai86** Roger Y. Tsai, *An efficient and accurate camera calibration technique for 3D machine vision.*, Proceedings of IEEE Conference on Computer Vision and Pattern Recognition, 1986, pp. 364-374.
- Walter97** Bruce J. Walter, Philip M. Hubbard, Peter Shirley, and Donald P. Greenberg. *Global illumination using local linear density estimation*, ACM Transactions on Graphics, 1997 (to be published).

Acknowledgements

We are thankful to Bruce Walter for generating the synthetic image and to Steve Marshner for providing us a tool to carry out the camera pose calibration and for his help during the measurements. This work was supported by the NSF Science and Technology Center for Computer Graphics and Scientific Visualisation (ASC-8920219) and by NSF Metacenter Regional Alliance (ASC-9523483), and performed on workstations generously donated by the Hewlett-Packard Corporation.

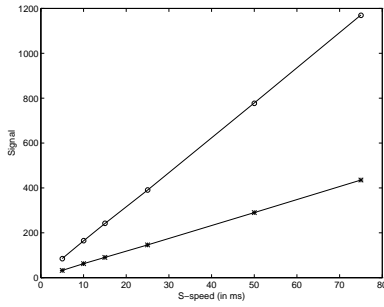


Figure 1: Signal as a function of exposure time.

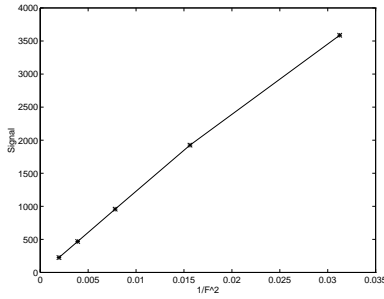


Figure 2: Signal as a function of F-stops.

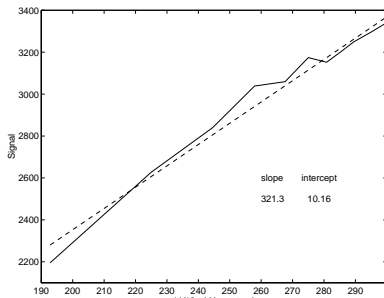


Figure 3: Signal as a function of image distance.

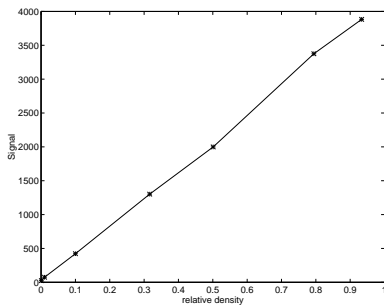


Figure 4: Signal as a function of Photon flux.

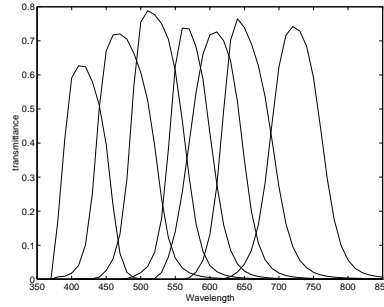


Figure 5: Transmittance curve of the 7 Filters.

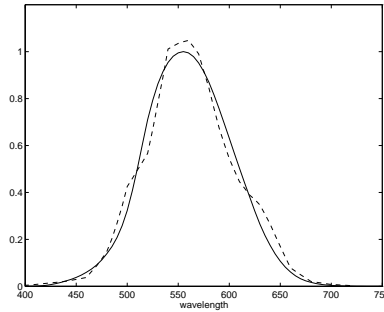


Figure 6: Reconstructed $\bar{y}(\lambda)$ function (dotted line) superimposed on actual $\bar{y}(\lambda)$ function (solid line).



Measured Image



Computed Image



Difference Image (scaled)

Figure 7: Comparison.